15th World Congress on Computational Mechanics (WCCM-XV)
8th Asian Pacific Congress on Computational Mechanics (APCOM-VIII)
Virtual Congress: 31 July – 5 August 2022
S. Koshizuka (Ed.)

WIND PRESSURE CHARACTERISTICS OF HIGH-RISE BUILDINGS IN MIDDLE AND HIGH-HEIGHT URBAN AREAS SPREAD OVER LOCAL TERRAIN

KOJI KONDO[1], HIDENORI KAWAI[2], TETSURO TAMURA[3] AND KEIGO NAKAJIMA[4]

[1]Kajima Corporation
2-19-1 Tobitakyu, Chofu-shi, Tokyo, Japan
kondokoj@kajima.com

[2]Ochanomizu University
2-1-1 Otsuka, Bunkyo-ku, Tokyo, Japan
kawai.hidenori@ocha.ac.jp

[3]Tokyo Institute of Technology
2-12-1 Ookayama, Meguro-ku, Tokyo, Japan
tamura.t.ab@m.titech.ac.jp

[4]Kajima Corporation
2-19-1 Tobitakyu, Chofu-shi, Tokyo, Japan
nakakeig@kajima.com

Key words: Wind Pressure Characteristics, High-rise Building, Local Terrain, Inflow Turbulence

Abstract. *In an urban area where middle and high-height buildings are densely built on a complex terrain, it is important for wind-resistant design to know what kind of strong wind blows during a typhoon and the wind pressure acts on the building. In this study, we focused on the wind of the wind direction SSE observed during typhoon LAN (2017), and investigated the relationship between the topography and the flow field around the buildings, and the wall surface pressure by LES. As a result, we clarified the complicated flow due to the interference between the target building and the local terrain and surrounding buildings. In addition, the validity was shown by comparing the wind pressure coefficient of LES with that of the wind tunnel experiment.*

1 INTRODUCTION

In the wind resistant design of buildings, it is necessary to consider the influence of surroundings such as the local terrain and buildings. At that time, it is important to reproduce the characteristics of the turbulent boundary layer. In this paper, the influence of the urban area spreads over the windward area of the target building was investigated by giving the velocity fluctuation obtained by LES (Large Eddy Simulation) of the wider urban area to the inflow boundary condition. The relationship between the wind flow field around buildings and the wall surface pressure was clarified by LES. Based on these results, we report the effects of local terrain and adjacent buildings, as well as the characteristics of wind pressure acting on the uniquely shaped façade.

2 FEATURES OF AKASAKA AREA

Akasaka area, which is adjacent to the green areas such as Akasaka Palace, Hie-shrine, and Sotobori, is densely built with middle and high-rise buildings over the local terrain as shown in Figure 1. Figure 2 shows the contour maps of the elevation of the local terrain. The height difference of the local terrain is about 20m. Many high-rise buildings are located at Kasumigaseki and Roppongi areas on the SSE to SE directions of Akasaka area.

Figure 1: Feature of Akasaka area

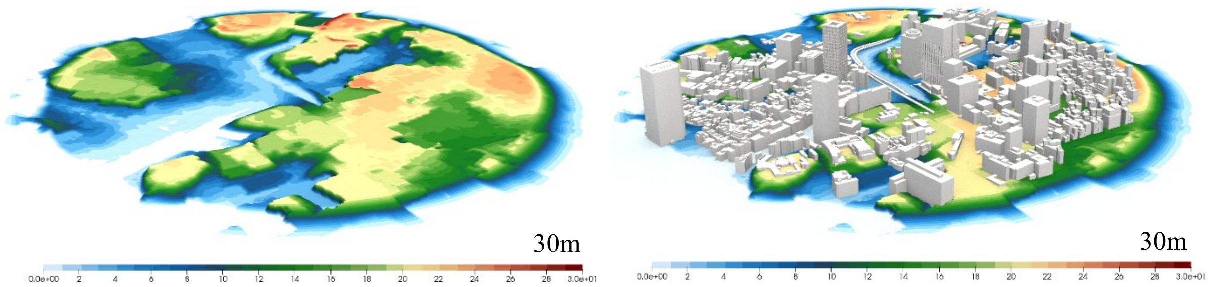

(a) Local terrain (b) Local terrain with buildings

Figure 2: Contour maps of elevation of local terrain

3 COMPUTATIONAL MODEL

Figures 3 and 4 show the computational model of LES. The computational model reproduces the local terrain and buildings in a range of 1.2 km in diameter centered on the intersection of Akasaka-mitsuke. In addition, the height difference at the outer edge is rubbed on GL 0m within a range of 1.5 km in diameter. The size of the computational area is 2km in width, 2km in depth and 1km in height. There are four distinctive buildings in this area. Building A (47.5m(width) ×47.5m(depth) ×154.5m(height)) has the girder-shaped outer frame. Building B (58.7m×58.7m×148.7m) is the tri-star shape high-rise building, and a same size high-rise building is located in close proximity. Building C (70.2m×70.2m×161.0m) has the wavy façade divided into four blocks in the height direction, and there is the semi-outdoor space passage in the lower part. In addition, there is the steep slope to Sotobori adjacent to it. Building D (43.4m×41.8m×159.0m) is adjacent to the hill leading from Hie-shrine.

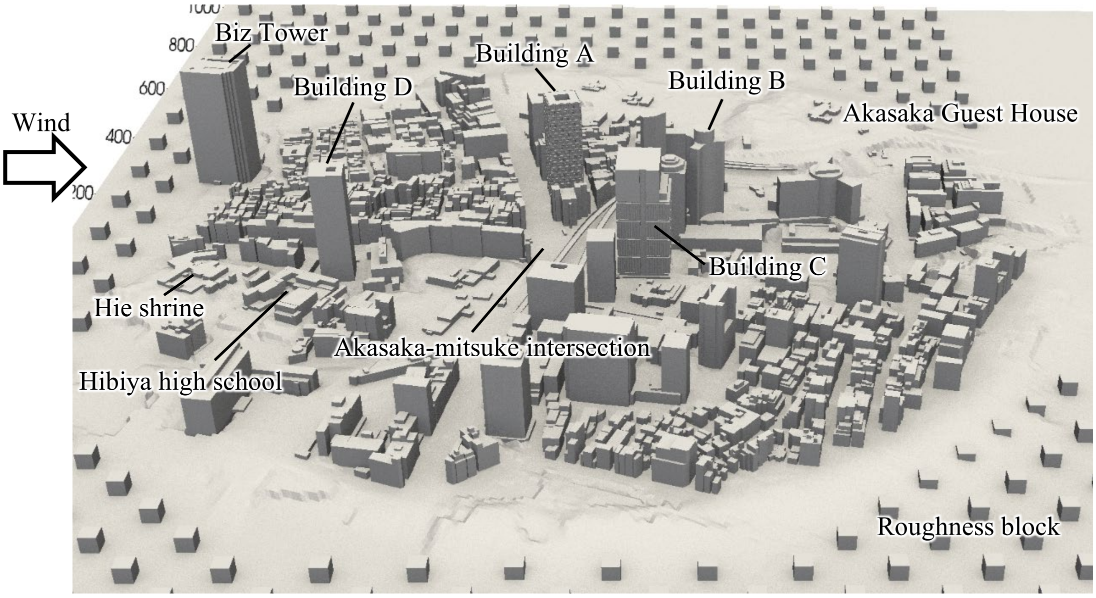

Figure 3: Computational model of Akasaka area

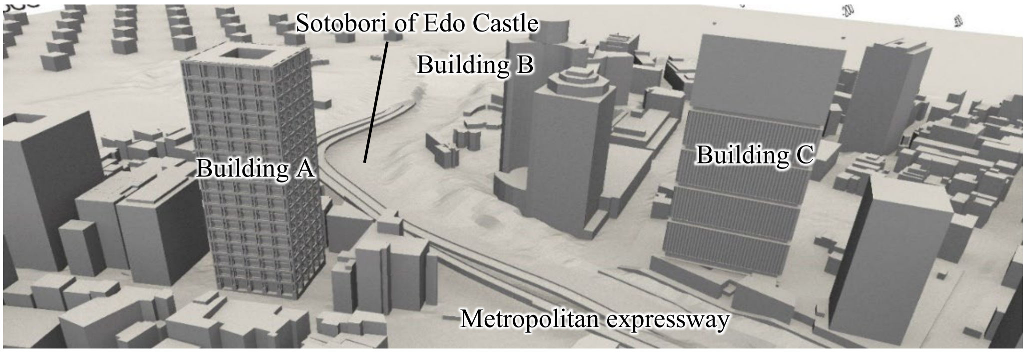

Figure 4: Computational model (Enlarge view of buildings A, B and C)

4 CALCUATION METHOD

4.1 Calculation method

The incompressible BCM (Building Cube Method) fluid analysis code CUBE developed by RIKEN is used for the analysis [1]-[3]. This code uses a method based on a multi-step structured grid (BCM), and by arranging cubes with exactly the same calculation load on the same number of processors, the load balance is equalized and high calculation performance is demonstrated.

Efficient use of the hierarchical cache using the characteristics of the structured grid makes it possible to improve the performance of a single processor. One cube is divided into 16×16×16 grids. Basic grid resolution on the surface of the ground and buildings is set to 1m over the whole area so that the influence of the local terrain and buildings can be grasped everywhere, and the immersed boundary condition is applied to the boundary surface. The grid resolution of 0.5m is used around Buildings A, B, C and D. The total number of grids is about 347 million. The layouts of cube in the computational domain are shown in Figures 5 and 6. In this study, we focus on the wind direction SSE observed during Typhoon Lan (2017). SGS model is dynamic model.

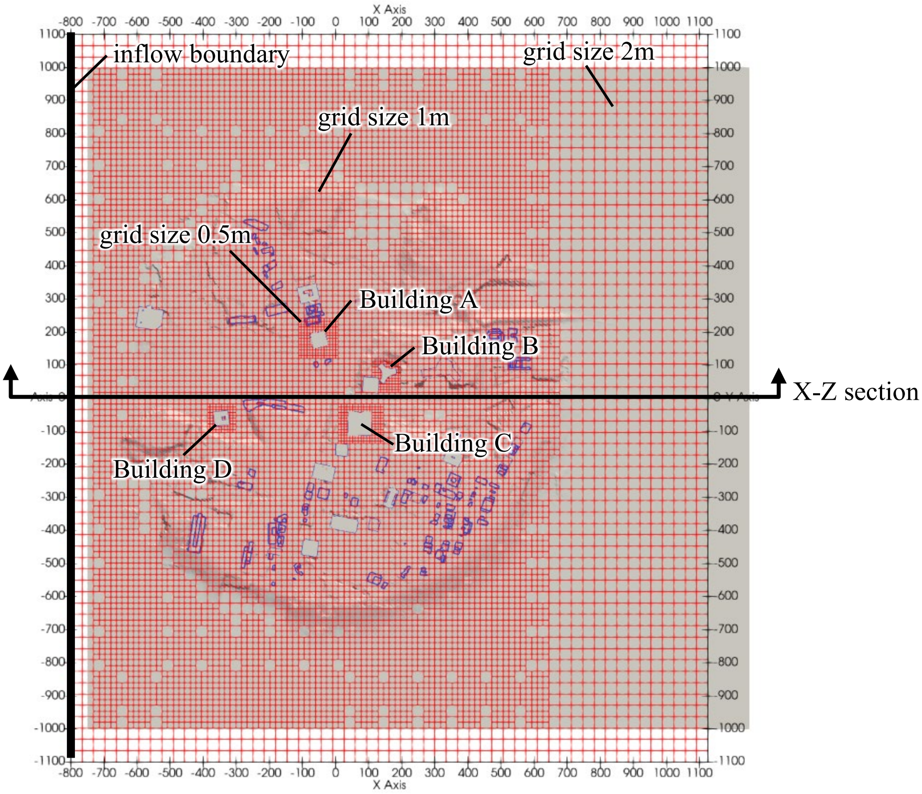

Figure 5: Layout of cube in X-Y plane (Z=50m)

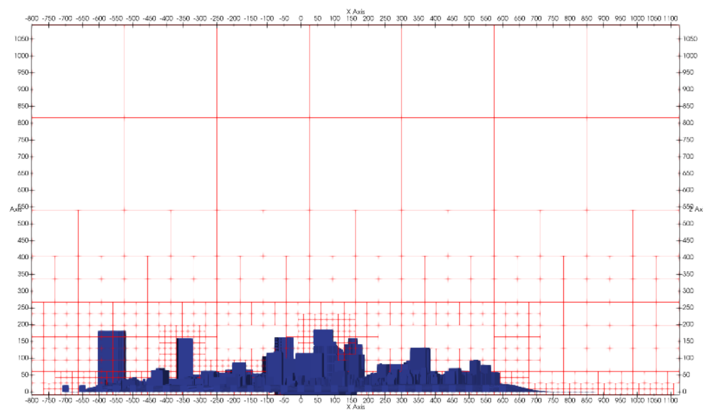

Figure 6: Layout of cube in X-Z plane (Y=0m)

4.2 Boundary condition

The inflow turbulence obtained by the meteorological analysis and LES for wider area is applied to the inflow boundary condition of LES [4]. The vertical profiles of the inflow turbulence at seven points in spanwise are shown in Figure 7 in comparison with the vertical profiles of the power law index of 0.27 [5]. The vertical profiles of the inflow turbulence vary in spanwise, but the variation is not so large. Compared with the profile of the power law index α=0.27 of the terrain category IV shown in the AIJ Guideline [5], the inflow turbulence is a more developed boundary layer which has the larger mean wind velocity gradient and a larger fluctuating wind velocity. In this calculation, the wind velocity is converted so that the Reynolds number of 65574. The boundary condition is shown in Table 1.

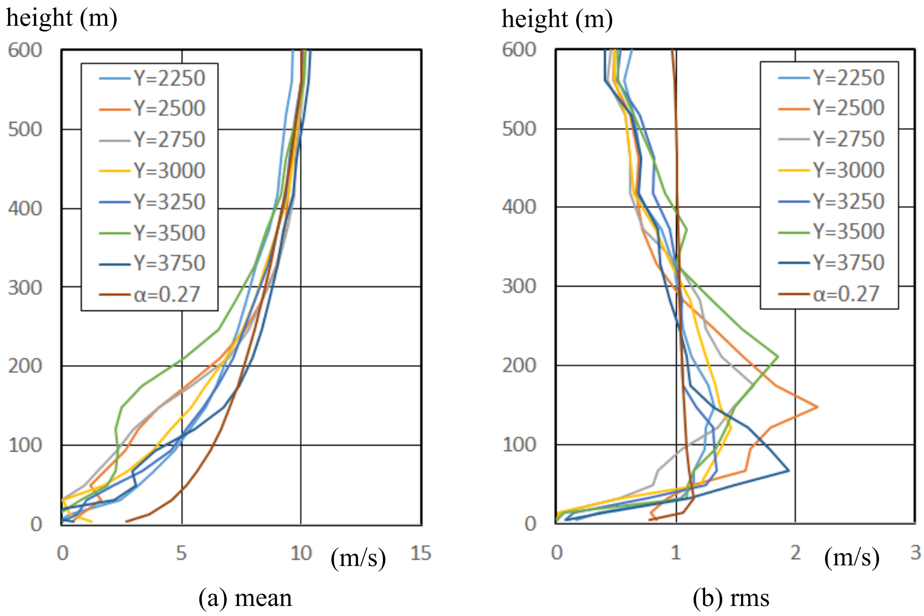

Figure 7: Vertical profiles of inflow turbulence [4], [5]

Table 1: Boundary condition

inflow	inflow turbulence
outflow	convective type
floor	non-slip
object surface	immersed boundary method (IBM)
side wall	free-slip
upper wall	free-slip

5 CALCULATION RESULTS

5.1 Flow field around Akasaka area

Figure 8 shows the instantaneous flow field in the horizontal section around Akasaka area at the height of 50m. Figure 9 is an enlarged view of the instantaneous flow field in the horizontal section around Buildings B and C. And Figure 10 shows the instantaneous flow field in the vertical section around the Buildings A and C. The wind velocity increase areas can be seen around Buildings A, B, C and D.

The streamlines around the target buildings calculated from the mean wind velocity filed are shown in Figure 11 to confirm the flow field in detail. Looking at Figure 11(b), it can be seen that the wind flow affected by Biz Tower on the windward side acts on the Building A. The wind blowing through Sotobori-dori acts on building B and the adjacent building, but the distance between these two buildings is narrow, there are not much streamlines between them (see Figure 11(c)).

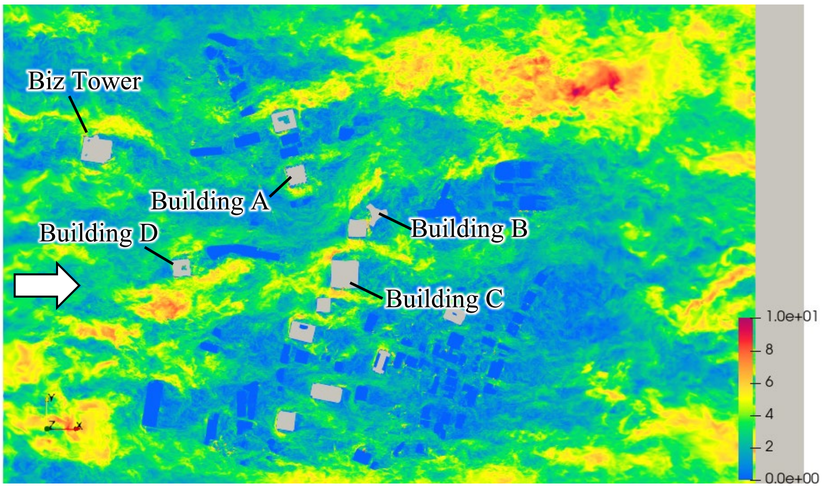

Figure 8: Instantaneous flow field in horizontal section around Akasaka area (Z=50m)

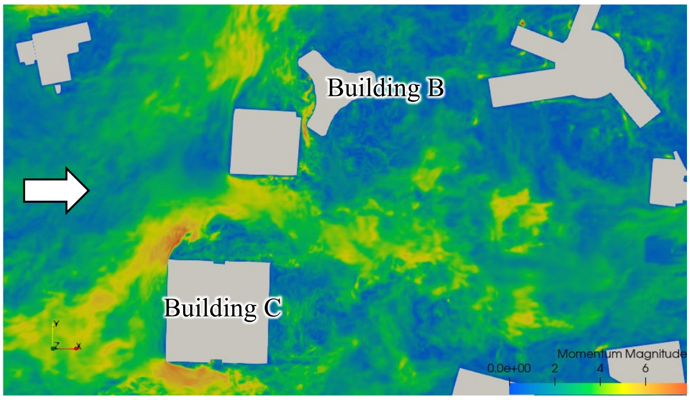

Figure 9: Instantaneous flow field in horizontal section around Buildings B and C (Z=40m)

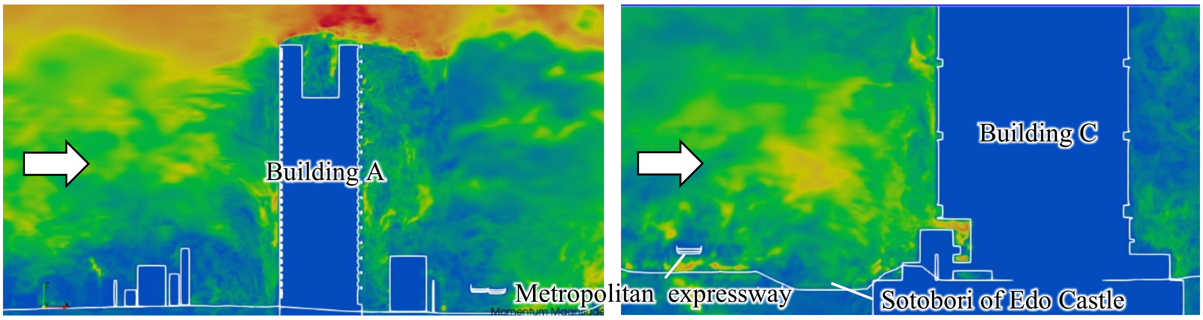

(a) Building A (b) Building C

Figure 10: Instantaneous flow fields in vertical section around Buildings A and C

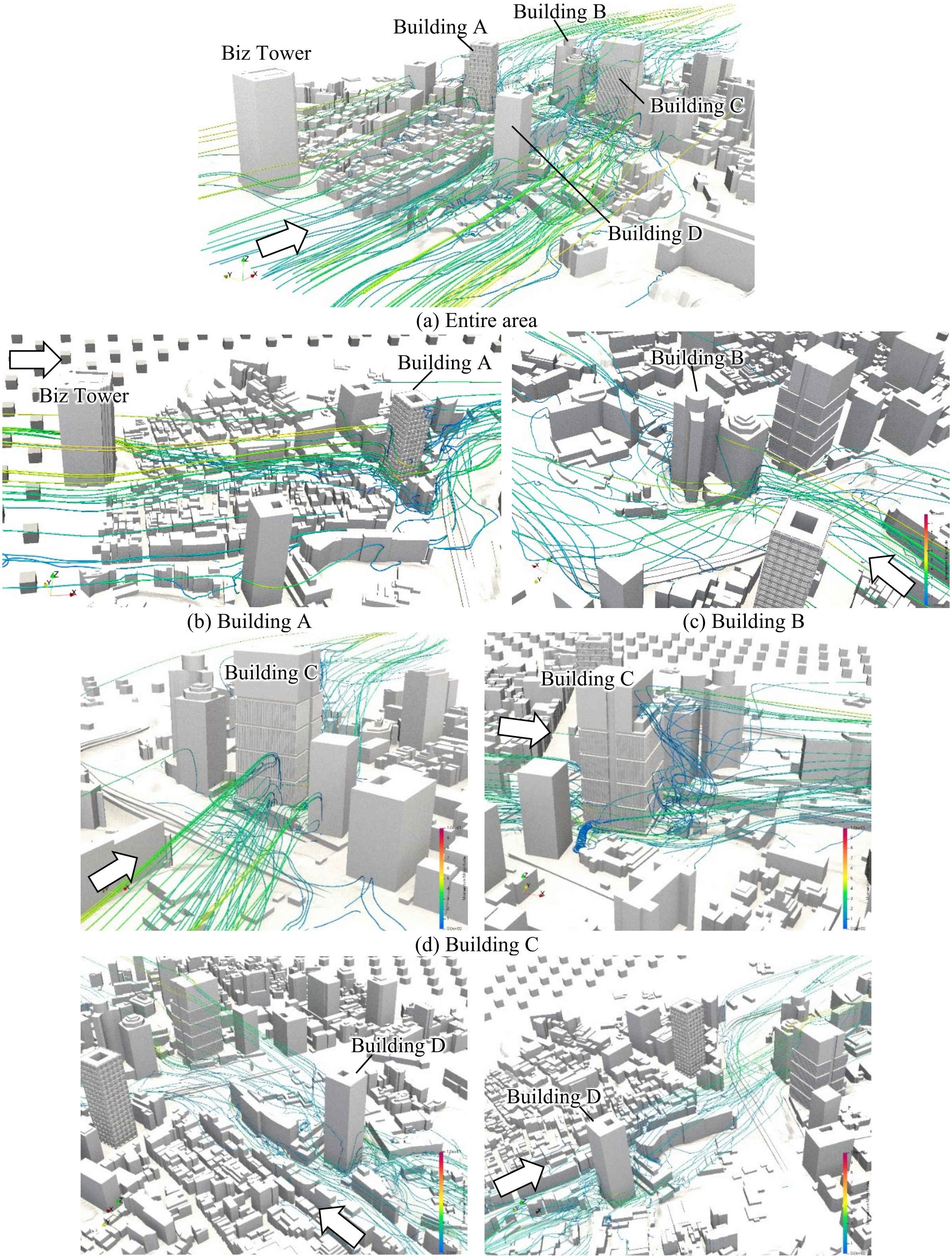

(a) Entire area

(b) Building A

(c) Building B

(d) Building C

(e) Building D

Figure 11: Streamlines of mean wind velocity around Buildings A, B, C and D

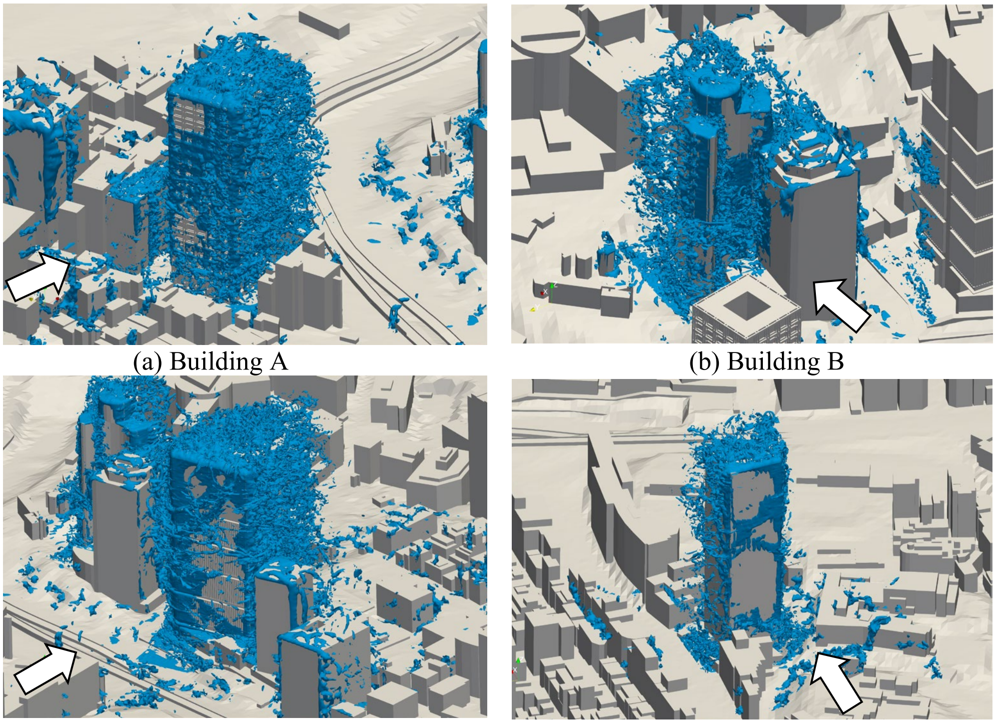

(a) Building A (b) Building B

(c) Building C (d) Building D

Figure 12: Instantaneous distributions of vorticity around buildings A, B, C and D

Looking at Figure 11(d), the flow from the windward side hill crosses above Sotobori, impinges the middle height of Building C, and blows down to the lower part of the building. On the other hand, the flow from the windward side hill blows down to Sotobori and blows up the slope of Sotobori again then impinges the lower part of Building C. These flows are blown up behind Building C and flow away to the wake. Looking at Figure 11(e), the flow from Hie-shrine hill impinges the middle height of Building D, and blows down to the lower part of the building. Around the lower part of Building D, the flow converges among Hibiya high school hill or adjacent buildings. This flow is blown up over the buildings and the hills behind Building D and flows toward Building C.

Figure 12 shows the instantaneous distributions of vorticity around Buildings A, B, C and D. Around Building A, fine vortex structures can be seen not only on the side walls and wakes, but also on the windward surface due to the complex façade of the building surface. Around Building B, the complex vortex structure can be seen due to the interference of the separation flow from the windward side high-rise building [4].

6 COMPARISON OF WALL SURFACE PRESSURE

In order to verify the reproducibility of the wind pressure, the wind pressure coefficients on the wall surface of Building A are compared with those of the wind tunnel experiment. Figure 13 shows the position of probe points and Figure 14 shows the distribution of the mean wind pressure on Building A surface calculated by LES. Figure 15 shows the correlation between the wind pressure coefficients of LES and those of the wind tunnel experiment. LES is the results of the wind direction of 157.5 degree, and the wind tunnel experiment is the results of wind directions of 155 degree and 160 degree.

There are some variations in the average, maximum, and minimum values due to the difference in the evaluation time between LES and the wind tunnel experiments, but they show generally good agreement. On the other hand, the rms value is larger in LES. This is because, as shown in Figure 7, the wind velocity fluctuation of the inflow turbulence obtained by the wide area LES is larger than those of the wind tunnel experiment with the power law index α=0.27. Furthermore, there are some points of poor matching, but this is because the minimum grid resolution of 0.5m is coarse to reproduce the shape of the outer frame of Building A. This point will be confirmed in the calculation using the finer grid resolution in the future.

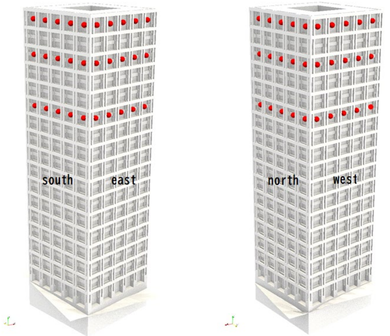

Figure 13: Position of probe points on Building A surface

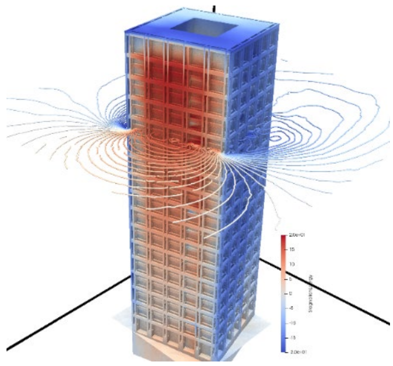

Figure 14: Distribution of mean wind pressure coefficient on Building A surface (LES)

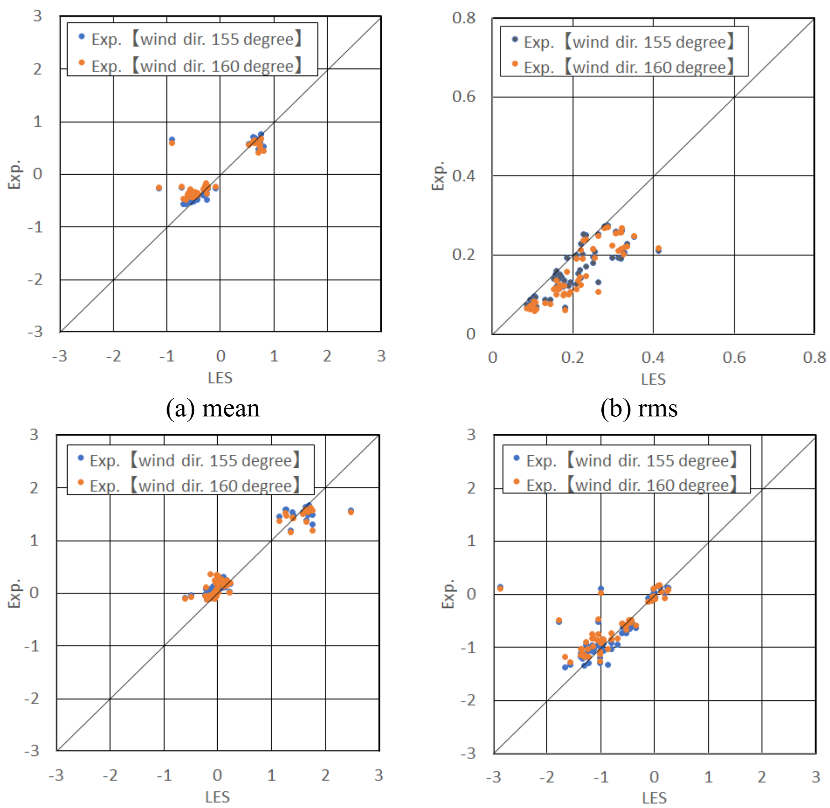

(a) mean (b) rms

(c) maximum (d) minimum

Figure 15: Comparisons of wind pressure coefficients on Buildings A wall surface

7 CONCLUSIONS

- In this study, we focused on the wind of the wind direction SSE observed during typhoon LAN (2017), and investigated the relationship between the topography and the flow field around the buildings and the building wall pressure by LES.
- As a result, we clarified the complicated flow due to the interference between the target buildings and the local terrain and surrounding buildings. In addition, the validity was shown by comparing the wind pressure coefficient by LES with the results of the wind tunnel experiment.
- In the future, we will investigate the relationship between the flow field and the wall surface wind pressure in more detail. In addition, we plan to improve the accuracy of the wind pressure prediction by using higher grid resolution.

8 ACKNOWLEDGMENTS

The result of this research was obtained from “Smart design in the Society 5.0 era on the supercomputer Fugaku” which was the 2021 HPCI priority use category theme of RIKEN (program number: hp210262). I would like to express my gratitude here.

REFERENCES

[1] Tetsuro Tamura, Hidenori Kawai, Rahul Bale, Keiji Onishi, Makoto Tsubokura, Koji Kondo and Tsuyoshi Nozu, Analysis of wind turbulence in canopy layer at large urban area using HPC database, ICUC9-9th International Conference on Urban Climate jointly with 12th Symposium on the Urban Environment (2015).

[2] Tetsuro Tamura, Hidenori Kawai, Kazuaki Uchibori, Rahul Bale, Keiji Onishi, Makoto Tsubokura, Koji Kondo and Tsuyoshi Nozu, High performance computation by BCM-LES on flow and pressure field around buildings, 8th International Colloquium on Bluff Body Aerodynamics and Applications, Northeastern University, Boston, Massachusetts, USA, 7 – 11 June (2016).

[3] Koji Kondo, Tetsuro Tamura, Hidenori Kawai, Makoto Tsubokura, Keiji Onishi, Rahul Bale and Kahoru Nakayama, Characteristics of turbulent boundary layer developed over wide city area, 30th Computational Fluid Dynamics Symposium, Japan, (2016). (in Japanese)

[4] Hidenori Kawai, TetsuroTamura and Masaharu Kawaguchi, LES on wind pressure acting on high-rise building under strong wind events of Typhoon, 15th World Congress on Computational Mechanics (WCCM-XV) 31 July - 5 August (2022).

[5] Architectural Institute of Japan, Recommendations for Loads on Buildings (2015).